Molecular Dynamics Simulation of Nanosized Water Droplet Spreading in an Electric Field

ARTICLE *in* LANGMUIR · MARCH 2013

Impact Factor: 4.46 · DOI: 10.1021/la304763a · Source: PubMed

3 AUTHORS, INCLUDING:

Fenhong Song
University of Michigan-Dearborn
4 PUBLICATIONS **25** CITATIONS
SEE PROFILE

Chao Liu
Chongqing University
71 PUBLICATIONS **397** CITATIONS
SEE PROFILE

Langmuir

Article

pubs.acs.org/Langmuir

Molecular Dynamics Simulation of Nanosized Water Droplet Spreading in an Electric Field

F. H. Song,[†,‡] B. Q. Li,*[,§] and C. Liu[†]

[†]Key Laboratory of Low-Grade Energy Utilization Technologies and Systems of Ministry of Education, Chongqing University, Chongqing 400030, China

[‡]School of Mechanical Engineering, Xi'An Jiaotong University, Xi'An, Shaanxi 710049, China

[§]Department of Mechanical Engineering, University of Michigan, Dearborn, Michigan 48128, United States

ABSTRACT: Molecular dynamics (MD) simulations are performed for the spreading of a nanosized water droplet on a solid substrate subject to a parallel electric field. A combined electrostatic and Lennard–Jones potential is employed to represent the intermolecular interactions. Results show that in response to the applied field, polar water molecules realign themselves and this microscopic reorientation of molecular dipoles combines with the intermolecular forces to produce a macroscopic deformation of a free spherical water droplet into an ellipsoid. The applied field has a strong effect on the spreading of the water droplet on a solid substrate. For a weaker parallel field, the droplet spreading is asymmetric with the leading contact angle being greater than the trailing contact angle. With an increase in field strength, this asymmetry continues to increase, culminates, and then decreases until it disappears. The symmetric spreading remains with a further increase in the field strength until the saturation point is reached. This transition from the asymmetric to symmetric spreading is a manifestation of the interaction of the electric field with polar water molecules and the intermolecular forces within the droplet and between the water and solid; the interaction also leads to a change in hydrogen bonds along the droplet surface. The dynamics of the droplet spreading is entailed by the electrically induced motion of molecules along the liquid surface toward the solid substrate and is controlled by a competing mechanism among the electric, water–water, and water–solid intermolecular forces.

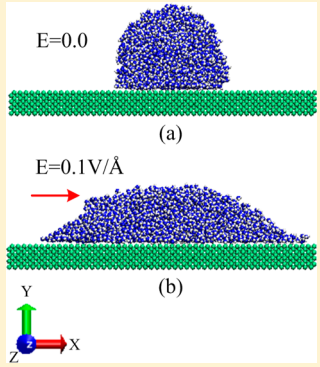

1. INTRODUCTION

Use of an electric field to control the liquid–solid contact behavior is found in a wide range of thermal and micro/nanoelectromechanical systems: from the enhancement of film boiling to the manipulation of a tiny droplet with electrowetting.[1,2] The presence of the electric field is known to affect the liquid bubble nucleation and evaporation during boiling, leading to an increase in local heat transfer efficiency. Interaction of a droplet with an external electric field forms the basis for many microelectronic and nano-optoelectronic technologies, such as inkjet printing,[3] electrostatic painting and spraying,[4,5] and nanoimprinting and nanomanufacturing.[6,7] These existing and, in particular, the emerging applications in nanotechnology have generated much research interest in developing a better understanding of localized interaction between liquid molecules and solid surfaces as facilitated by an external electric field.[8−10]

In macroscopic systems, the effect of an applied electric field on liquid spreading on a solid surface is known to be described by the celebrated macromechanical Young–Lippmann equation,[11]

$$\cos\theta = \frac{\gamma_{sg} - \gamma_{sl}}{\gamma_{lg}} + \frac{\langle \varepsilon\varepsilon_0 \mathbf{E}\cdot\mathbf{E}\rangle D}{2\gamma_{lg}} \quad (1)$$

where θ is the contact angle, D the thickness of the interfacial double layer,[8] γ the surface tension, $\mathbf{E}$ the applied electric field, ε the dielectric constant of the liquid, and ε_0 the dielectric constant of free space. Also, the subscripts l, g, and s refer to the liquid, gas, and solid, respectively, and the angular bracket stands for the average over D. Measurements on a water drop on a solid surface show that the above equation is valid up to the saturation point.[11]

For microscopic systems, molecular dynamics simulations provide a useful tool for analysis. MD studies have shown that the Young–Lippmann equation generally does not hold true for the spreading behavior of a droplet of nanosize in an electric field.[8−10] Novel liquid–solid contact phenomena emerge when a nanosized liquid drop spreads over a solid surface in an applied electric field.[10] These derivations are attributed to the large surface-to-volume ratio in a nanosized liquid and the hydrogen bonds near the solid–liquid–vapor triple point. A comprehensive review of recent work on the electrocapillary/electrowtting phenomena associated with a liquid column or a droplet in contact with the solid surface is given by Daub et al.[9] The MD simulations obtained by Daub et al.[8] illustrate that for a nanosized droplet, the liquid–solid contact angle is related

Received: December 1, 2012
Revised: March 13, 2013
Published: March 14, 2013

   dx.doi.org/10.1021/la304763a | *Langmuir* 2013, 29, 4266–4274

not only to the polarity of the applied field but also to the direction of the field. For an electric field applied parallel to the solid surface, the liquid spreads on the surface asymmetrically with the leading contact angle differing from the trailing one. This is in direct contrast with eq 1, which suggests that the contact angle is determined solely by the magnitude of the electric field. Using MD simulations, Yen[10] further studied the solid−liquid contact angle of a nanosized drop on a solid surface subject to an applied electric field perpendicular to the solid surface and found that the liquid−solid contact angle depends both on the polarity of the applied field and on the field strength. The MD results[10] further reveal that for a perpendicular field, the contact angle first decreases and then increases as the field strength increases, and also the magnitude of the change in the contact angle is different when the polarity switches for the same field strength.

While the existing studies revealed certain important nanoscale features that differ significantly from the macroscopic description, some important fundamental issues concerning the microscopic mechanism of the field effect on a nanodroplet spreading on a solid surface remain unanswered. For example, it is known now that a nanosized drop spreads asymmetrically in an electric field parallel to the solid surface,[8] but how this asymmetric spreading depends on the applied field strength has yet to be fully appreciated. In fact, our MD simulations presented below demonstrate that for a parallel field, the asymmetry between the leading and trailing contact angles exists only up to a certain critical value of electric field strength, beyond which the asymmetry disappears and the droplet spreads symmetrically onward until the saturation point is reached. In addition to that, an understanding also is needed of how water molecules dynamically respond to the applied field and rearrange themselves accordingly to result in asymmetric and then symmetric spreading as the field strength increases.

This paper presents an MD study of a nanosized droplet in contact with a solid substrate subject to an electric field applied in parallel to the solid surface. The solid has a cubic diamond structure. The spreading asymmetry is studied by examining the dynamic process of the liquid droplet spreading on the surface driven by the parallel field. MD simulations for the deformation of a free droplet are also presented. The microscopic mechanism of the effect of a parallel electric field on the deformation of a nanosized water droplet and its static contact angle on a solid substrate is interpreted in light of MD simulations. Information presented below on the molecular details of droplet deformation and spreading in an electric field should be of great value to enhance our fundamental understanding of the microscopic physical mechanisms governing the electric field interaction with a droplet in contact with a solid surface.

2. MOLECULAR MODELS AND SIMULATION DETAILS

A simple point charge/extension (SPC/E)[12] water model was used as a basis for MD simulations. The molecule (SPC/E model) takes a tetrahedral shape with two hydrogen atoms connecting to the oxygen atom through covalent bonds. Hydrogen is positively charged, while oxygen is negatively charged. Table 1 lists the parameters for the model used for calculations. The intermolecular interactions are calculated as follows. The electrostatic interaction is modeled using Coulomb's law, while the dispersion and repulsion force using the Lennard−Jones (L−J) potential,[12,13]

Table 1. Parameter of SPC/E Water Model

r(OH) (Å)	1.0
HOH (deg)	109.47
q(O)	−0.8476
q(H)	0.4238

$$\phi(r_{ij}) = 4\varepsilon_{oo}\left[\left(\frac{\sigma_{oo}}{r_{oo}}\right)^{12} - \left(\frac{\sigma_{oo}}{r_{oo}}\right)^{6}\right] + \frac{1}{4\pi\varepsilon_0}\sum_{i=1}^{3}\sum_{j=1}^{3}\frac{q_i q_j}{r_{ij}} \quad (2)$$

where the L−J potential is applied only for oxygen−oxygen interaction, with σ_{oo} = 3.166 Å and ε_{oo} = 0.1556 kcal/mol. The last term in eq 1 describes the Coulomb force between the charged atoms, where q_i is the charge on atom i; r_{ij} is the distance between atoms i and j, and ε_o is the dielectric constant for a vacuum. In our studies, it is normalized as 1.

The interaction between the water and solid substrate is modeled by the modified L−J potential of the following form,

$$\phi_{ls}(r_{ij}) = 4\varepsilon_{ls}\left[\left(\frac{\sigma_{ls}}{r_{ij}}\right)^{12} - \left(\frac{\sigma_{ls}}{r_{ij}}\right)^{6}\right] \quad (3)$$

where ϕ_{ls} is the potential energy between the liquid and solid, and σ_{ls} and ε_{ls} are the distance and the energy parameters, respectively. They are calculated according to the Lorentz−Berthelot mixing rule,[14]

$$\varepsilon_{ls} = \sqrt{\varepsilon_l \varepsilon_s}\,\sigma_{ls} = (\sigma_l + \sigma_s)/2.0 \quad (4)$$

For a silicon solid substrate, σ_{ls} = 0.3278 nm and ε_{ls} = 0.301 kcal/mol. A smooth cutoff is used for the interatomic pair potentials. As the droplet is of finite size and the solid substrate carries no charges, the use of Ewald sums is not needed.[8,17] Repeated tests show that a cutoff radius of 15 Å is satisfactory for the present study.

When an external electric field E is present, an additional force $f_{ie} = q_i E$ is exerted on each atom according to its charge q_i. The detail of the treatment is given elsewhere,[15] which was followed by the present study.

The solid substrate has a cubic diamond structure. The droplet has 2000 water molecules initially stacked in a simple spherical structure at the center of the simulation box. This is equivalent to a spherical drop in radius of 2.5 nm and is large enough for a MD simulation (see Accuracy of Simulation and Density Distribution). The size of the simulation box was set as 140 × 140 × 140 Å. Studies[16] show that a time step of 5 fs or less gives a good accuracy. For the results presented below, a time step of 2 fs was used, which gives sufficiently accurate results for a moderate computational cost.

Unlike others who started with a cubic structure of water and evolve the structure to an equilibrium droplet shape,[17−19] we started directly with a droplet of perfect sphericity, which is obtained through a separate MD simulation with gravity neglected. To do so, the initial velocities are assigned to the atoms randomly, according to the system's temperature. Periodic boundary conditions are applied in all directions. The system is allowed to reach equilibrium at which a spherical droplet forms. An electric field is then added to investigate the electrically induced deformation of the droplet from its initial spherical shape. In the case of spreading, the initial spherical drop is first allowed to come into contact with the solid substrate, and then the electric field is applied. This approach

dx.doi.org/10.1021/la304763a | Langmuir 2013, 29, 4266−4274

appears to be less time-consuming than starting with a cube of water.

For the MD simulations presented in this paper, the solid substrate consists of 10816 solid atoms arranged in diamond cubic lattice, with a lattice constant of 5.46 Å. This is one of the solid silicon structures. The solid substrate is rigid. Figure 1 shows the ensemble structure with the initial spherical drop of 2000 water molecules obtained from a separate MD simulation.

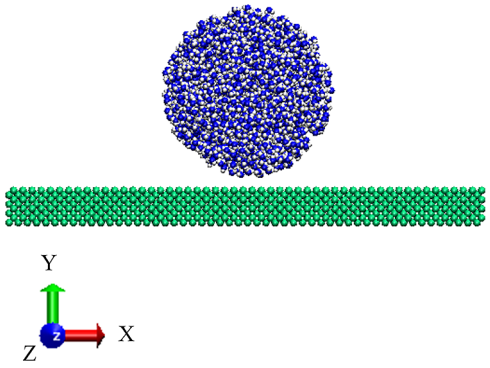

Figure 1. Initial structure of the ensemble.

To simulate the droplet spreading on a solid surface, periodic boundary conditions are applied along the x and z directions. In the y (i.e., vertical) direction, the mirror boundary condition is specified at the top surface; that is, if the atom reached the boundary, the x- and z-velocity components remain the same, while its y component changes signs. The bottom surface of the box is fixed with the solid surface.

The Nose Hoover thermostat,[20,21] which relaxes the temperature in a timespan of 100 time steps, was used at every time step to ensure that the ensemble is at a desired temperature. Figure 2 shows the potential energy and the total

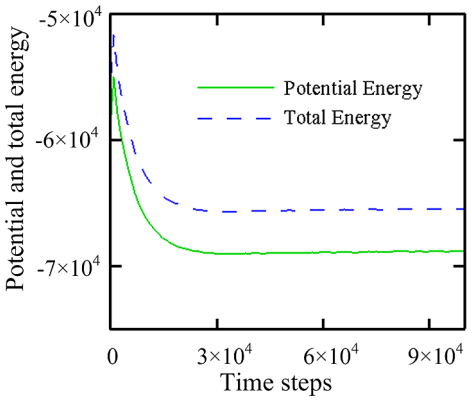

Figure 2. The variation of potential and total energy with time.

energy distribution of the system as a function of time steps for a typical simulation. Clearly, the system reached an equilibrium state after ~50000 time steps. In the results presented below, the system first was allowed to continue up to 100000 time steps to ensure a good equilibrium state. Afterward, sampling was taken at every 50 time steps to obtain the statistically averaged values for the next 100000 time steps. This was applied to obtain the shape of a free drop as an initial condition. An electric field then was imposed in either the x or the y direction, where the x direction is parallel to the plate and the y direction upward (see Figure 1). Additional 100000 time steps were used for the system to reach a new equilibrium and afterward sampling is taken for analysis.

Under the electric field, water droplet density is sampled by dividing the simulation domain into 140 × 140 × 140 small cubes. The water droplet density contour is obtained from the density profile. The ellipse function was fitted using the least-squares method from points on the droplet contour. Figure 3

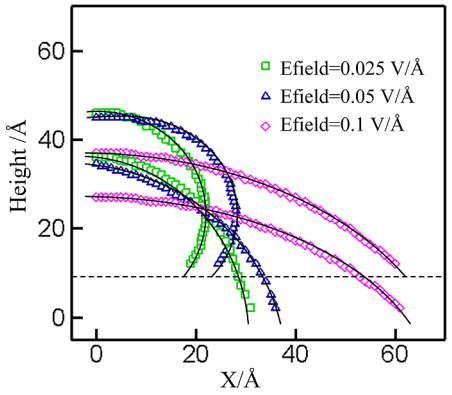

Figure 3. Water droplet contour for different electric fields: solid lines are the elliptical cross sections fitted with simulation data marked by symbols.

shows the fitted ellipse function and the data points for various electric fields. This is different from other approaches,[22,23] where the surface contour of a droplet is fit to a circle. Simulations show that the shape of a water droplet on the plate is more like part of an ellipsoid than a spherical crown, especially with the presence of an external electric field.[8] The contact angle is then obtained from the tangent line, according to the ellipse function.

3. ACCURACY OF SIMULATION AND DENSITY DISTRIBUTION

For MD simulations, a sufficient number of molecules are needed to obtain an accurate statistical representation of a system. To obtain the needed information on the number of molecules required, simulations were conducted with different numbers of molecules in the presence or absence of an external electric field, and the density function distribution was then obtained. The results of a free droplet without an imposed electric field are shown in Figure 4 for MD simulations using 500, 1000, 2000, 3000, 4000, and 5000 water molecules. Inspection of the results reveals that a simulation with 2000 molecules or more should yield an accurate statistical representation, which is consistent with that used in literature.[8−10]

4. RESULTS AND DISCUSSION

4.1. Effect of the Parallel Electric Field on Liquid Spreading. Liquid spreading on a solid surface is characterized by contact angles, the interpretation of which has been a subject of intensive research in recent years without[22−28] and with an applied electric field.[1−3] Here, MD simulations are presented to analyze the effect of an electric field on the spreading of a nanosized droplet on a solid substrate. The effect of the field applied perpendicularly to the solid surface has been analyzed;[10] here, the focus is on the effect of the parallel field. Toward this end, the MD simulations were carried out

dx.doi.org/10.1021/la304763a | Langmuir 2013, 29, 4266−4274

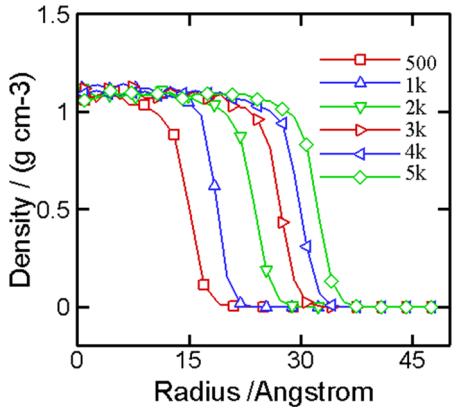

Figure 4. Density profile with different number of water molecules in the droplet.

with electric field strengths of 0.0, 0.025, 0.05, 0.075, 0.1, and 0.15 V/Å. The data show that without an electric field, the droplet spreads symmetrically on the substrate with a contact angle of 86.47°, which is consistent with the experimental data reported in literature.[29]

Figure 5 depicts the difference between the leading and trailing contact angles as a function of the parallel electric field

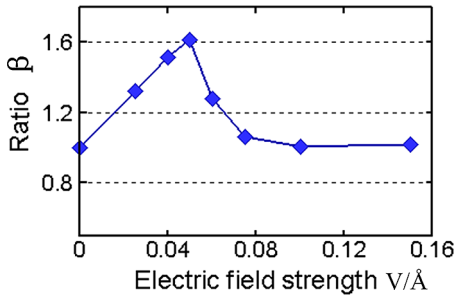

Figure 5. The ratio β of the leading over trailing contact angles as a function of the electric field strength.

strength. The leading and trailing contact angles refer to the left and right contact angles, when a field is applied from the left to the right (see also Figure 7). Clearly, the asymmetry of the leading and trailing contact angles depends on the field strength. As the field strength increases, the asymmetry increases until it reaches a maximum and then starts to decrease. The asymmetry disappears and the leading and trailing contact angles become the same as the field strength further increases. This rather nonlinear effect may be attributed to the combined effect of an applied electric field, the hydrogen bonding, the intermolecular forces, and the interaction between the water molecules and the solid surface.

In the absence of the electric field, the molecular motions are random but statistically symmetric. This leads to the same leading and trailing contact angles. When a weak electric field is applied, the polar water molecules tend to orient themselves along the electric field, with the oxygen atoms (negatively charged) against, and the hydrogen, along the field direction. The reorientation caused by the electric field loosens some hydrogen bonds on the liquid surface above the solid substrate. Hydrogen bonds are considered to have direct relevance on the contact angles.[30] From the simulation data, the orientation distributions (that is, the dipole moment and OH bond vector) of water molecules were obtained (see Figure 6 for some

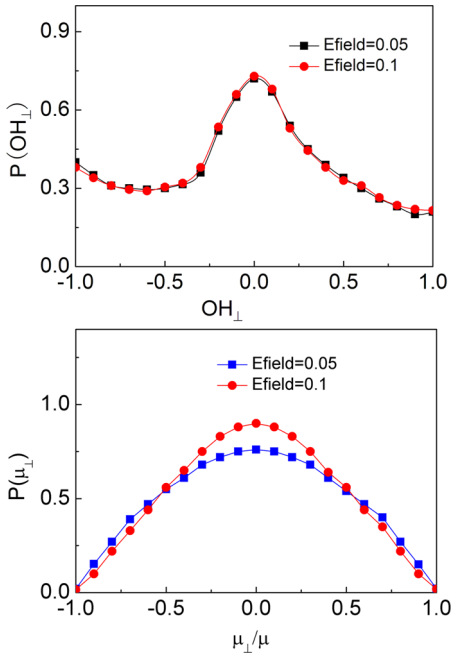

Figure 6. Distribution of perpendicular components of the OH bond vector (upper) and the water molecular dipole moment vector (lower) near the liquid–solid interface in the presence of electric fields, E = 0.05 and 0.1 V/Å.

selected cases) and are analyzed, along with the mean hydrogen bonds per molecule near the leading and trailing edges. These data are in qualitative agreement with the calculations reported in literature,[8,30] indicating that the normal component of water molecules is essentially unaffected by the parallel fields. From these data, the following picture is constructed. In a field-free case, the HOH plane tends to be perpendicular to the plane of the vapor/water interface, with one OH bond vector pointing out of the interface toward the vapor phase.[31] Near the solid surface, the water molecules have their dipoles aligned along the surface.[8,32] With the field applied pointing from the left to the right as shown in Figure 5, when the water molecules are rotated and pulled away from the surface by the electric field, hydrogen atoms are moved toward it into the water to form more hydrogen bonds with molecules inside the surface. Near the right surface of the droplet, however, the hydrogen atoms that were statistically bonded with internal oxygen atoms through hydrogen bonding are also reduced because the realignment of the water molecules with the field will likely cause more some hydrogen atoms to move away from the interface. Because interfacial tension increases with a decrease in hydrogen bond numbers,[8] the interfacial tension γ_{lg} at the left side (the leading edge) is larger than the right side (the trailing edge). Since a breakup of one solid–liquid bond leads to the creation of a new solid–vapor bond, the difference, $\gamma_{sl} - \gamma_{sg}$, is affected approximately equally at both the leading and trailing edges. At the same time, near the solid surface, the weaker electric field is not strong enough to overcome the solid–water interaction to move the polar water molecule along the field direction. Thus, the molecules in the first layer above the solid basically remain at the same location, though they may rotate to tend to align with the field. This is indicated by the fact that the normal component distribution of the dipole moment and OH bond vector of these molecules in the parallel fields is similar to that without a field (these orientation data are

dx.doi.org/10.1021/la304763a | Langmuir 2013, 29, 4266–4274

very similar to those reported;[8,32] see also Figure 6). The solid−liquid interaction becomes smaller for water molecules away from the solid surface. Consequently, more hydrogen bonds are broken along the right-side water surface from the solid toward the top of the droplet, while the opposite occurs along the left-side surface, thereby resulting in unequal leading and trailing contact angles.

As the field increases, the above asymmetry between the leading and trailing contact angles is further skewed because of a competing mechanism between the field stretching effect and the other restricting forces. The stronger field produces a higher degree of reorientation of the polar molecules, and at the same time, the intermolecular forces and solid−liquid forces are still strong enough to constrain the motion of the molecules.

With the electric field strength further increased, the larger leading contact angle tends to increase, and at some point, the water molecules on the liquid surface above the solid become unstable. These molecules are then pulled onto the solid surface by the solid−liquid intermolecular forces, thus spreading the liquid along the surface and producing a net result of reducing the leading contact angle. For an even stronger field, the electric force becomes predominant, causing polar water molecules to almost completely align with the electric field. This in turn yields a statistically symmetrical droplet shape because the large parallel electric field stretches the water droplet in both directions, causing it to wet the solid surface equally. As a result, the asymmetry between the leading and trailing contact angles disappears. This is also consistent with the results on hydrogen bond data obtained from simulations in the present study. For example, at E = 0.05 V/Å, the mean hydrogen bond numbers in the solid−liquid regions are 2.702 and 2.776 for the leading and trailing edges, respectively, but the corresponding hydrogen bond numbers in the liquid−vapor regions are 2.832 and 2.713. This suggests a smaller γ_{lg} and thus a larger leading contact angle, since $\gamma_{sl} - \gamma_{sg}$ is affected equally on both sides.[8] In contrast, at E = 0.1 V/Å, the mean hydrogen bond numbers in the solid−liquid regions are 2.831 and 2.837 for the leading and trailing edges, respectively, and the corresponding numbers are 2.622 and 2.624, which clearly suggest a symmetric spreading, that is, the leading and trailing contact angles being the same.

Figure 7 illustrates the equilibrium shapes of the droplet spreading on a solid surface for a parallel field of three different strengths. The view is projected onto the plane parallel to the applied electric field. In the absence of the electric field, the droplet spreads symmetrically on the substrate. A weak parallel field deforms the liquid asymmetrically along the field direction, with the leading contact angle differing from the trailing one. This is consistent with the result reported in literature,[8] which discussed this phenomenon for one field value. The results here further show, however, that the asymmetry occurs only for a weak field range. As the field strength increases beyond a point, the asymmetry reduces and then disappears and the deformation becomes symmetric. The deformation in the z direction (i.e., the direction into the paper) is, however, symmetric for all field values, as expected.

To further understand the effect of the applied field, the leading (i.e., the left-side) and trailing (i.e., the right-side) contact angles are plotted as a function of the field strength in Figure 8. These results reveal that as the electric field increases in strength, the asymmetry first becomes more noticeable, continues to reach a culmination, and then starts to decrease; eventually the asymmetry disappears at some point (E = 0.1 V/Å for this case). The liquid then continues to spread symmetrically with a further increase of the applied field.

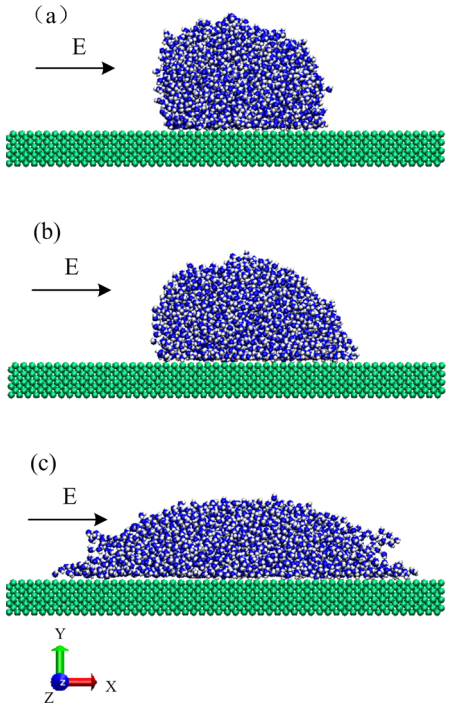

Figure 7. The equilibrium shapes of a water droplet spreading on a solid surface by a parallel field: (a) 0.025, (b) 0.05, and (c) 0.15 V/Å.

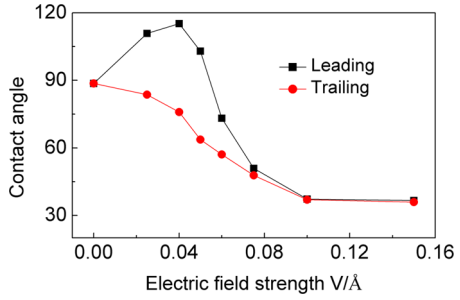

Figure 8. The dependency of leading and trailing contact angles upon the applied electric field: diamonds for the leading contact angle and circles for the trailing.

4.2. Dynamic Process of Spreading. To gain physical insight into the fundamentals governing the spreading of a nanodroplet on the solid in the parallel electric field, the dynamic spreading process of the droplet is examined for a case where the final equilibrium shape is symmetric. A set of the snapshots of the droplet spreading dynamics is shown in Figure 9, and the corresponding contact angles during the dynamic spreading are plotted in Figure 10. The dynamic contact angle is obtained as the average value for 10 snapshots, extracted every 50 time steps around a time point. For these calculations, the initial condition is the equilibrium state of a water droplet spread onto the solid surface without an electric field. Then, an electric field parallel to the solid surface and with the strength to cause a final symmetric spreading is introduced. It is seen that the onset of the applied electric field causes the droplet to deform asymmetrically, with the leading contact angle being larger than the trailing one. The deformation evolves with time, gradually becomes symmetric as the spreading continues, and remains so hereafter until it reaches the final equilibrium state.

dx.doi.org/10.1021/la304763a | Langmuir 2013, 29, 4266−4274

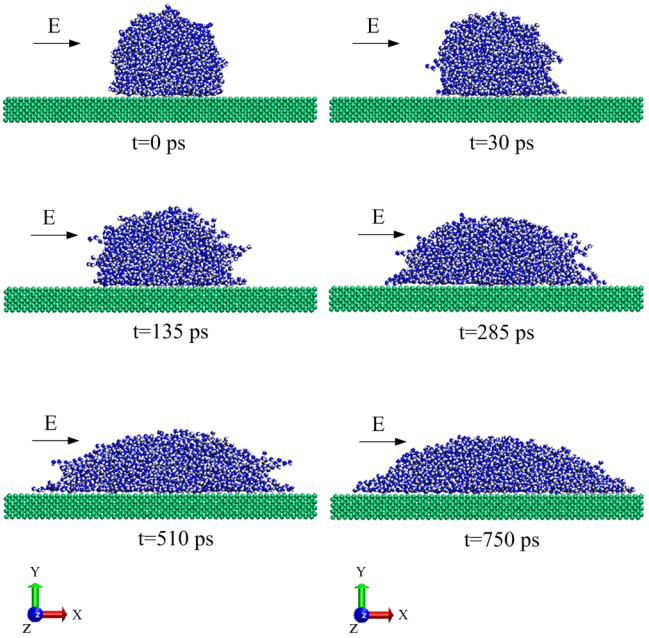

Figure 9. Dynamic spreading of a water droplet onto the solid surface with the presence of an electric field (E = 0.1 V/Å).

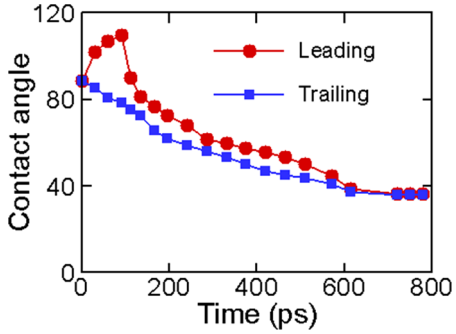

Figure 10. Dynamic leading and trailing contact angles during electrically induced spreading of the water droplet (field strength = 0.1 V/Å).

Here, the droplet responds to the applied field by initially realigning the water droplets, in a very similar fashion as discussed above. The initial response is such that the molecules away from the solid surface tend to rotate and move toward the electric field, which causes the drop to deform asymmetrically. The continuous rotation and realignment of the molecules along the electric field eventually stretch the droplet symmetrically. From the results, it is seen that the leading contact angle experiences a brief increase and then decreases as the droplet deformation evolves in an electric field, whereas the trailing contact angle decrease continuously as the droplet deforms in response to the applied electric field.

As discussed above, the realignment of the molecules by the applied electric field affects the hydrogen bonding between molecules in the interface region, which in turn affects γ_{sl} and γ_{lg}. For the cases of parallel electric fields under the present study, the orientation distributions of water molecules and the mean hydrogen bond data were obtained from the simulation data at various time steps. The orientation distribution data are similar to those discussed above in reference to Figure 5. Near the solid surface region, these water molecules are predominately affected by the solid–liquid interactions and the water dipole moments are practically decoupled from the parallel field. Analysis of the data also reveals that the number of hydrogen bonds near the trailing edge differs from that near the leading edge, with the latter being larger than the former. For example, our data show that at time (ps) = 90, the mean number of hydrogen bonds (HB) near the liquid–vapor interface is 2.806 for the leading edge and 2.718 for the trailing edge. This means that the γ_{lg} is smaller at the leading edge, causing further departure from 90°. On the other hand, at time = 800 (ps), the mean HB numbers near the liquid–vapor interface for leading (2.624) and trailing (2.622) are about the same, suggesting a larger departure from 90° and a symmetric spreading. This is observed in Figure 10.

4.3. Motion of Molecules during Electrowetting. Examining the dynamic process also allows us to understand the microscopic mechanism by which the liquid molecules spread in response to an applied electric field. For this purpose, three different water molecules at three different locations in the drop are monitored for their path trajectories during the electrically induced spreading process. The three molecules are chosen as follows: one at the surface far away from the solid surface, one close to the surface, and one just on the surface. The results are shown in Figure 11. It is seen that the molecule just on the surface, denoted by C, moves randomly on the surface but remains practically around its initial position during spreading. The molecule on the liquid surface away from the solid, A, however, moves along the surface and eventually deposit onto the solid. The movement of molecule B is similar to that of A. Once the molecule is deposited on the solid surface, however, the solid–liquid interaction constrains its motion. The molecule then behaves similarly to molecule C. These dynamic events suggest that the liquid spreading in the electric field undergoes the following phases. First, the water molecule rotates and orients itself in response to the electric field and some of the hydrogen bonds on the liquid surface are broken or broken during the process. The rotation and alignment continue until all the molecules have aligned with the electric field, if the field strength is strong enough. Then, the polar water molecules on the liquid surface start to move, with the molecules right above the surface to move toward the solid and deposit on the solid surface. Once they are on the surface, they become constrained by the solid–liquid interaction and remain randomly moving around a fixed position. The molecules far away from the solid then move along the liquid surface toward the solid surface. The replenishing process continues to wet the solid until a saturation point is reached.

4.4. Deformation of a Droplet in an Electric Field. Macromechanical analysis shows that an applied electric field induces a nonuniform surface charge distribution along the surface of a water droplet. These induced surface charges further interact with the electric field to produce an electric force, which causes the droplet to deform, and the equilibrium shape of the deformation is determined by the balance of the surface tension and the normal component of electric stress tensor, if gravity is neglected.[33] Here, we explore the microscopic mechanism of this electric field induced droplet deformation at the molecular level. A free spherical droplet consisting of 2000 water molecules was considered as the starting point for the MD simulations. An external electric field with the value of 0.05 V/Å then was introduced to obtain a new equilibrium state. The snapshots of the water droplet in equilibrium states with and without an applied field are contrasted in Figure 12. The shape of a free water droplet in the

dx.doi.org/10.1021/la304763a | Langmuir 2013, 29, 4266–4274

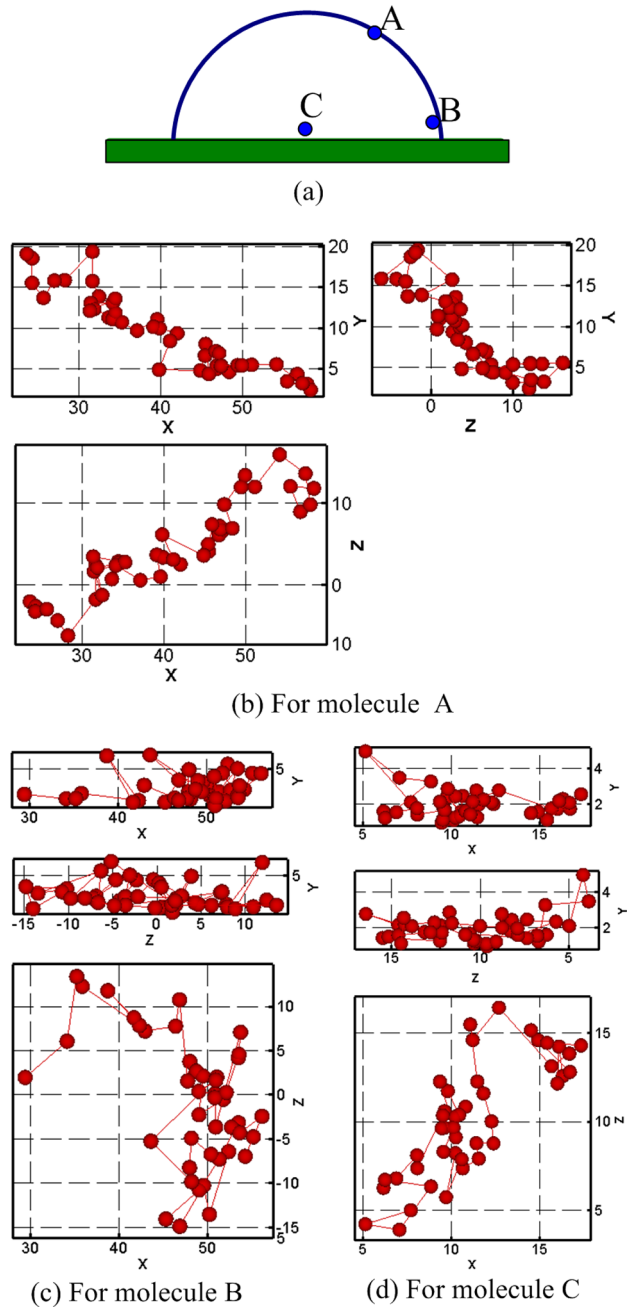

Figure 11. Trajectories of three water molecules during the spreading of a droplet by an electric field (E = 0.1 V/Å): (a) schematic of initial positions of the three molecules, (b) the time-evolving x, y, and z coordinates of molecule A during the spreading, (c) the time-evolving x, y, and z coordinates of molecule B, and (d) the time-evolving x, y, and z coordinates of molecule C.

equilibrium state in the absence of an external electric field assumes a spherical shape, as expected, while it deforms to an ellipsoid with an external electric field imposed, where the long axis of the ellipsoid is parallel to the electric field.

A water molecule is polar such that electrons are clouded more around the oxygen atom than the two hydrogen atoms bonded to it. As a result, in a water molecule, the hydrogen atoms tend to have a slightly positive charge (i.e., electropositive) and the oxygen atoms a slightly negative charge (i.e., electronegative), causing the water molecule to behave like a point dipole. In the absence of an external electric field, the

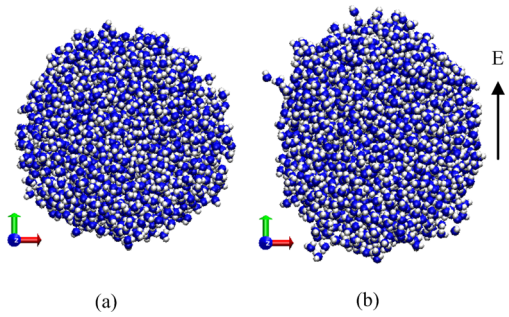

Figure 12. Snapshot of a water droplet under an electric field (E = 0.05 V/Å): (a) the equilibrium state of a water droplet without an electric field and (b) the equilibrium state of a water droplet with the electric field in the y direction.

point dipole is randomly oriented in accordance with the intermolecular forces among the water molecules. Consequently, a free droplet is spherical in shape at statistical equilibrium. With an applied electric field, the interaction between the field and the point dipole tends to orient the dipole along the field direction. Thus, for the applied field pointing upward, a water molecule rotates itself such that the two electropositive hydrogen atoms are on the top and the electronegative oxygen atom at the bottom. The reorientation action causes these dipoles to shift along the electric field, producing a net stretching action on the water droplet. On the other hand, the intermolecular forces between the water molecules will restore themselves into the equilibrium random orientations associated with a free droplet, once the water dipoles are deviated from their equilibrium positions. The balance of the above electric forces and the intermolecular forces eventually results in the final equilibrium shape of a droplet being ellipsoidal, as shown in Figure 12b.

On the surface of the water droplet, the molecules are less constrained by the intermolecular forces than those inside and, thus, the molecular dipoles are more easily oriented along the direction of the electric field. At equilibrium, the electropositive atoms appear on the upper half surface of the ellipsoid-shaped water droplet, while the electronegative is on the lower half. This is also confirmed by a cut view of the middle plane (z = 0) of the equilibrium shape. These microscopic arrangements produce a nonuniformly distributed macroscopic surface charge such that the surface charges increase in magnitude along the surface from the equator toward the two poles. These surface charges interact with the applied electric field to produce a stretching force that pulls the water droplet apart in the upper and lower directions. This action is then counterbalanced by the surface tension effect. As a result, the macroscopic deformation of a water droplet takes an ellipsoidal shape.

Our MD simulations further show that for a weaker electric field, the droplet also deforms asymmetrically with the lower surface being flatter. The physical origin is the same as for the droplet spreading on the solid surface, except that in this case the solid−water interaction is absent; as a result, the strength of the applied field to transit from asymmetric to symmetric deformation is smaller than the droplet of the same size on a solid substrate.

5. CONCLUDING REMARKS

This paper has presented an MD study of the electric field effect on the deformation of a nanosized water droplet and the spreading of the droplet on a solid substrate. Molecular

dx.doi.org/10.1021/la304763a | Langmuir 2013, 29, 4266−4274

interactions are represented by an intermolecular potential that combines the electrostatic and L−J potentials. A droplet consisting of 2000 molecules appears to give good accuracy. An external electric field interacts with a polar water molecule to reorient its point dipole. The microscopic reorientation of the molecular dipoles by the electric field is manifested by a macroscopic nonuniform distribution of induced charges on the droplet surface, which together with the electric field and the surface tension defines a macroscopic droplet deformation. The static contact angle of the water droplet on a solid substrate is affected by both the strength and the direction of an applied electric field. For a weaker parallel field, the droplet spreading is asymmetric with the leading contact angle being larger than the trailing contact angle. As the field strength increases, this asymmetry becomes more noticeable, reaches a maximum, and then decreases. A further increase in the field strength then leads to a symmetric spreading of the droplet until the saturation point is reached. This transition from the asymmetric to symmetric spreading is determined by a competing mechanism between the applied field, the intermolecular forces within the droplet, and between the water and the solid. These competing forces lead to the change in hydrogen bonds along the droplet surface and, hence, the liquid−solid contact behavior. Analysis of the spreading dynamics reveals that the applied electric field causes the water molecules to rotate and move along the surface of the droplet and to eventually deposit onto the solid surface, thereby leading to electrowetting. This is also consistent with the data of the water molecule orientation distributions and mean hydrogen bond numbers obtained from the present simulations.

AUTHOR INFORMATION

Corresponding Author

*E-mail: benqli@umich.edu. Tel: (+1)313-593-5241. Fax: (+1) 313-593-3851.

Author Contributions

The manuscript was written through contributions of all authors. All authors have given approval to the final version of the manuscript.

Notes

The authors declare no competing financial interest.

ACKNOWLEDGMENTS

The authors acknowledge the financial support of this work from the Oakridge University Research Alliance of the Department of Energy and Research Fund for the Doctoral Program of Higher Education (Grant 20090191110016).

REFERENCES

(1) Didkovsky, A. B.; Bologa, M. K. Vapour film condensation heat transfer and hydrodynamics under the influence of an electric field. *Int. J. Heat Mass Transfer* **1981**, *24* (05), 811−819.

(2) Bologa, M. K.; Korovkin, V. P.; Savin, I. K. Mechanism of condensation heat transfer enhancement in an electric field and the role of capillary processes. *Int. J. Heat Mass Transfer* **1995**, *38* (01), 175−182.

(3) Twardeck, T. G. Effect of parameter variations on drop placement in an electrostatic ink jet printer. *IBM J. Res. Dev.* **1977**, *21* (01), 31−36.

(4) Ku, B. K.; Kim, S. S. Electro hydrodynamic spraying characteristics of glycerol solutions in vacuum. *J. Electrost.* **2003**, *57* (1), 109−128.

(5) Barlettaa, M.; Gisario, A. Electrostatic spray painting of carbon fibre-reinforced epoxy composites. *Prog. Org. Coat.* **2009**, *64* (4), 339−349.

(6) Schaffer, E.; Albrecht, T. T.; Russell, T. P.; Steiner, U. Electrically induced structure formation and pattern transfer. *Letters to Nature* **2000**, *403* (24), 874−877.

(7) Liang, X. G.; Zhang, W.; Li, M. T.; Xia, Q. F.; Wu, W.; Ge, H. X.; Huang, X. Y.; Chou, S. Y. Electrostatic force-assisted nanoimprint lithography (EFAN). *Nano Lett.* **2005**, *5* (3), 527−530.

(8) Daub, C. D.; Bratko, D.; Leung, K.; Luzar, A. Electrowetting at the nanoscale. *J. Phys. Chem. C.* **2007**, *111* (2), 505−509.

(9) Daub, C. D.; Bratko, D.; Luzar, A. Nanoscale wetting under electric field from molecular simulations. *Top Curr. Chem.* **2012**, *307*, 155−179.

(10) Yen, T. Investigation of the effects of perpendicular electric field and surface morphology on nanoscale droplet using molecular dynamics simulation. *Mol. Simul.* **2012**, *38* (6), 509−517.

(11) Shamai, R.; Andelman, D.; Berge, B.; Hayes, R. Water, electricity, and between...On electrowetting and its applications. *Soft Matter* **2008**, *4*, 38−45.

(12) Berendsen, H. J. C.; Grigera, J. R.; Straatsma, T. P. The missing term in effective pair potentials. *J. Phys. Chem.* **1987**, *91* (24), 6269−6271.

(13) Kirby, B. J. *Micro- and Nanoscale Fluid Mechanics: Transport in Microfluidic Devices*; Cambridge University Press: Cambridge, U.K., 2010.

(14) Allen, M. P.; Tildesley, D. J. *Computer Simulation of Liquids*; Oxford University Press: Oxford, U.K., 1989.

(15) Park, S.; Schulten, K. Calculating potentials of mean force from steered molecular dynamics simulations. *J. Chem. Phys.* **2004**, *120* (13), 1651473.

(16) Streett, W. B.; Tildesley, D. J.; Saville, G. Multiple time-step methods in molecular dynamics. *Mol. Phys.* **1978**, *35* (03), 639−648.

(17) Werder, T.; Walther, J. H.; Jaffe, R. L.; Halicioglu, T.; Koumoutsakos, P. On the water carbon interaction for use in molecular dynamics simulations of graphite and carbon nanotubes. *J. Phys. Chem. B* **2003**, *107* (06), 1345−1352.

(18) Yang, T. H.; Pan, C.; Hsieh, H. M. In *Molecular Dynamics Simulation of Interactions between a Nano Water Droplet and an Isothermal Platinum Surface*, Proceedings of the 3rd IEEE International Conference on Nano/Micro Engineered and Molecular Systems, Sanya, China, Jan 6−9, 2008; IEEE, 2008.

(19) Hong, S. D.; Ha, M. Y.; Balachandar, S. Static and dynamic contact angles of water droplet on a solid surface using molecular dynamics simulation. *J. Colloid Interface Sci.* **2009**, *339* (1), 187−195.

(20) Hünenberger, P. H. Thermostat algorithms for molecular dynamics simulations. *Adv. Polym. Sci.* **2005**, *173*, 105−149.

(21) Yen, T. Wetting characteristics of nanoscale water droplet on silicon substrates with effects of surface morphology. *Mol. Simul.* **2011**, *37* (9), 766−778.

(22) Bertrand, E.; Blake, T. D.; Coninck, J. D. Influence of solid-liquid interactions on dynamic wetting: A molecular dynamics study. *J. Phys.: Condens. Matter* **2009**, *21* (46), 464124.

(23) Shi, B.; Dhir, V. K. Molecular dynamics simulation of the contact angle of liquids on solid surface. *J. Chem. Phys.* **2009**, *130*, 034705.

(24) Blake, T. D.; Clarke, A.; Coninck, J. D.; Ruijter, M. J. Contact angle relaxation during droplet spreading: Comparison between molecular kinetic theory and molecular dynamics. *Langmuir* **1997**, *13* (07), 2164−2166.

(25) Ingebrigtsen, T.; Toxvaerd, S. Contact angle of Lennard−Jones liquids and droplets on planar surface. *J. Phys. Chem. C.* **2007**, *111* (24), 8518−8523.

(26) Guo, H. K.; Fang, H. P. Drop size dependence of the contact angle of nanodroplets. *Chin. Phys. Lett.* **2005**, *22* (04), 787−790.

(27) Nieminen, J. A.; Abraham, D. B.; Karttunen, M.; Kaski, K. Molecular dynamics of a microscopic droplet on solid surface. *Phys. Rev. Lett.* **1992**, *69* (01), 124−127.

(28) Ohler, B.; Langel, W. Molecular dynamics simulations on the interface between titanium dioxide and water droplets: A new model for the contact angle. *J. Phys. Chem. C.* **2009**, *113* (23), 10189−10197.
(29) Suzuki, S.; Nakajima, A.; Yoshida, N.; Sakai, M.; Hashimoto, A.; Kameshima, Y.; Okada, K. Freezing of water droplets on silicon surfaces coated with various silanes. *Chem. Phys. Lett.* **2007**, *445*, 37−41.
(30) Bratko, D.; Daub, C. D.; Luzar, A. Water-mediated ordering of nanoparticles in an electric field. *Faraday Discuss.* **2009**, *141*, 55−56.
(31) Fan, Y.; Chen, X.; Yang, L.; Crème, P.; Gao, Y. Q. On the structure of water at the aqueous/air interface. *J. Phys. Chem. B.* **2009**, *113*, 11672.
(32) Shelley, J. C.; Patey, G. N. Boundary condition effects in simulations of water confined between planar walls. *Mol. Phys.* **1996**, *88* (2), 385.
(33) Song, S. P.; Li, B. Q. Free surface shapes and thermal convection in electro statically levitated droplets. *Int. J. Heat Mass Transfer* **2000**, *43*, 3589−3606.